Segmentation of Nuclear Medicine Three-Dimensional Images using Anscombe Transformation

Edward Flórez Pacheco, Sérgio Shiguemi Furuie

School of Engineering, University of São Paulo, Brazil

Abstract

In general, Nuclear Medicine images present poor signal to noise ratio mostly due to low counts and Poisson noise. The success of segmentation may be improved if relevant information of the input image is enhanced. Our aim was to verify segmentation improvement due to adequate filters. Basically, all images were submitted to Anscombe Transform, filtered by using Lee filter and inverse Anscombe Transform. Then, they were segmented by using Fuzzy Connected method and finally, compared to expected results. This study simulated real images obtained in Nuclear Medicine, such as the volume of the left ventricle of the heart (128x128x128 voxels), then Poisson quantic noise was incorporated in the simulation. For the assessment we used 30 three-dimensional images with different dimensions (volume, wall thickness) and different instances of Poisson noise, divided in three groups: Group I – 10 three-dimensional images of adult males, Group II – 10 three-dimensional images of adult females and Group III – 10 three-dimensional images of children. The analysis used the following parameters: True Positive (TP) rate and False Positive (FP) rate, and Maximum Distance (MaxDist) to the expected contour. Our results show consolidated results obtained from the validation of the image processing, by highlighting the usefulness of Anscombe/Lee filter, and showing the superiority of the segmentation values due to the proposed process.

1. Introduction

The use of PET modality as a medical imaging specialty is constantly growing and evolving [1]. One of the main characteristics that represents this kind of medical procedure, compared with other modalities that are currently being used for the obtaining of medical images is that PET has the capacity to provide biochemical anomalies of a particular body part that does not still represent an evident structural abnormality, which can generate an earlier diagnosis by experts [2].

The physical principles in PET image acquisition allow us to understand some important features of images generated, for instance, the intensities involved, noise associated with images that consequently degrade their quality. The objective of this work is to verify segmentation improvement due to adequate filters.

2. Methods

Processing an image consists in its manipulation through techniques aimed at extracting the information contained herein [5], having as a goal the improvement of visual information for human interpretation or for some specific application. For this purpose, we developed a complete 3D image processing as presented in the block diagram in Figure 1:

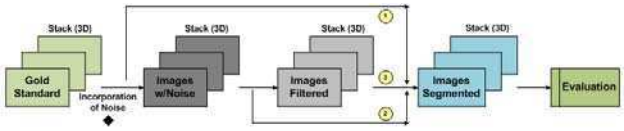

Figure 1. PET Images processing structure (3D)

Among the main elements of the processing structure, we have the following:

1. Acquisition or simulation of three-dimensional images of Nuclear Medicine;
2. Addition of quantum Poisson noise in the simulated three-dimensional images;
3. Three-dimensional image filtering;
4. Segmentation of structures of interest in three-dimensional images;
5. Process evaluation.

2.1. Acquisition or simulation of 3D images

The acquisition of an image is directly linked to the process of capturing and digitizing the image by using a specific method [3]. For our process, we tested different volumes of the Left Ventricle from simulations as follows:

Simulated left ventricle - Taking into account the dimensions and the main characteristics mentioned in the literature [2], we could simulate the cavity of the heart Left Ventricle as shown in Figure 2.

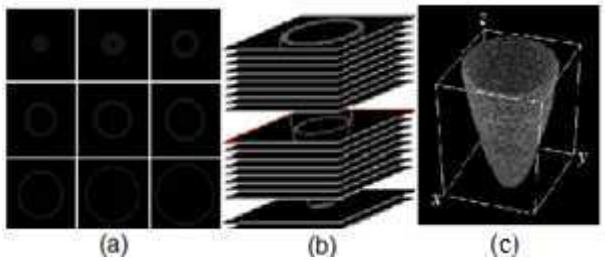

Figure 2. Simulation of the left ventricle of the heart. (a) projections of 2D slices of the left ventricle, (b) stack of 2D slices, (c) reconstruction of the volume of the left ventricle of the heart.

In Table 1 are listed the main parameters and their values considered in the elaboration of the simulated left ventricle. Based upon this initial model we generated a total of 30 volumes separated in three different groups: Group I – ten 3D images of males adult, Group II – ten 3D images of females adult and Group III – ten 3D images of children. Thus, keeping only the dimensions of the 3D matrix (128x128x128 voxels) we altered parameters such as left ventricular size (dimensions and wall thickness), the gray intensities of both the object and the background, and the Poisson noise which is randomly embedded in each of the slices that make up each of the simulated volumes.

Table 1. Main simulation parameters of the left ventricle.

Left ventricle simulated (parameters)	
Description	**Value**
width of the volume	128 pixels
height of the volume	128 pixels
depth volume	128 pixels
maximum distance x	60 pixels
maximum distance y	60 pixels
maximum distance z	80 pixels
wall thickness	12 pixels
background intensity	2
object intensity	20
distance between cuts	1 pixel
total slices generated	128

NCAT-4D phantom - We used some phantoms simulated with NCAT-4D [11]. Figure 3 shows the simulation of the Left Ventricle of the Heart along with structures of the ribcage (file name: ncat_lv60bpm_act_TOTAL.bin).

2.2. Addition of quantum Poisson noise

According to the literature, the PET images are affected by a quantum noise, which is dependent on the signal and can be represented by the statistical distribution of Poisson [8].

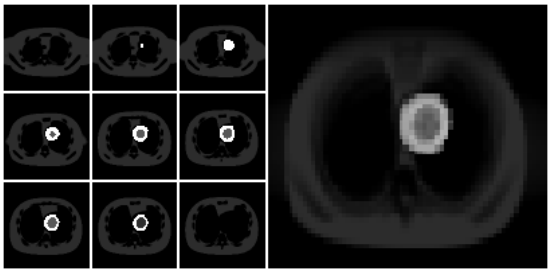

Figure 3. Phantom simulated using the 4D-NCAT. (a) projections of 2D slices of the left ventricle inside the ribecage, (b) volume generated with the ImageJ.

The volumes generated, from both the simulated left ventricle and the phantom NCAT-4D do not contain any kind of noise. Thus, as our objective is to process images close to real images, it is necessary for the gold standard images to adopt the main features of a real PET image. Then, incorporating Poisson noise on all input volumes is necessary.

2.3. Filtering 3D images

One of the processing techniques used to improve the quality of a digital image is the application of algorithms that eliminate unwanted noise in the image, usually generated in the acquisition process [5]. The approach proposed in this paper provides a restoration in the images utilizing, as a first step, the Anscombe Transform (AT) and the Lee filter to reduce the quantum noise. Afterwards, we used the Inverse Anscombe Transform (IAT) for the enhancement of the structures of interest in the filtered image.

Anscombe transform (AT) - The AT is a nonlinear transformation that allows to change the quantum noise of a digital image that is signal dependent into a noise approximately independent of the signal, additive, Gaussian, with zero mean and unit variance [8]. According to [6], given the random variable $\widetilde{U}_i$, with Poisson statistical distribution, we can express the Anscombe transform of this random variable by using the equation:

$$\tilde{Z}_i = 2 \cdot \sqrt{\widetilde{U}_i + \frac{3}{8}} \qquad (1)$$

This new variable $\tilde{Z}_i$, according to [8], can be represented by an additive model, as shown in the equation:

$$\tilde{Z}_i = 2 \cdot \sqrt{\widetilde{U}_i + \frac{1}{8}} + \widetilde{N}_i = \tilde{S}_i + \widetilde{N}_i \qquad (2)$$

with $\tilde{N}_i$ being a noise approximately independent of the signal $\tilde{S}_i$, described by a Gaussian distribution with zero mean and variance unit.

Lee filter - The Lee filter [7] is an optimal linear filter and can be used in the domain of Anscombe for filtering additive Gaussian noise. An estimate without noise $\hat{s}_i$ for $\tilde{Z}_i$ is obtained using the Lee filter given by the equation:

$$\hat{s}_i = E\left[\tilde{S}_i\right] + \frac{\sigma^2_{\hat{s}_i}}{\sigma^2_{\hat{s}_i}+1}\left(\tilde{Z}_i - E\left[\tilde{S}_i\right]\right) \qquad (3)$$

where the mean and the variance of $\hat{S}_i$, expressed respectively by $E\left[\tilde{S}_i\right]$ and $\sigma^2_{\hat{s}_i}$, are local measures and may be estimated in practice from the image to be filtered.

Inverse Anscombe transform (IAT) - After filtering the noise, we apply the inverse Anscombe transform in order to have an estimate of the degraded image without the quantum noise. We can express the IAT on $\hat{s}_i$ by the equation:

$$\hat{b}_i = \frac{1}{4}.\hat{s}_i^2 - \frac{1}{8} \qquad (4)$$

In Figure 4, we can visually distinguish the effect of the filtering step applied on the left ventricle, represented by the profiles of two-dimensional slices.

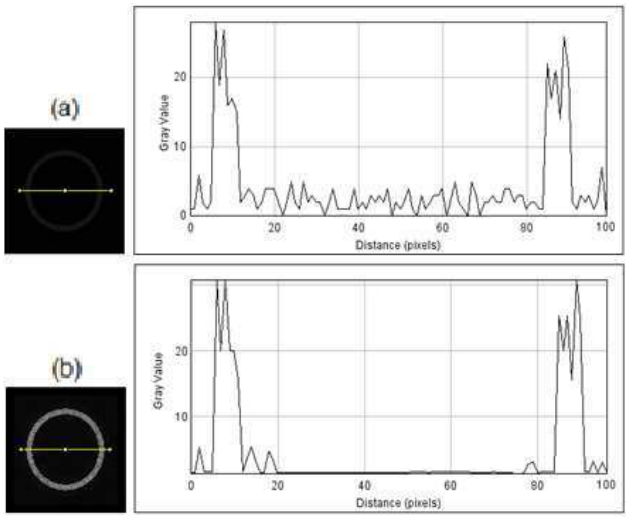

Figure 4. Profile (center horizontal line) of (a) Image with Poisson noise and (b) Image filtered.

2.4. Segmentation of 3D structures

The segmentation step in this work is based on the Fuzzy Connectedness theory using the dynamic weights approach [9]. The main characteristic of Fuzzy theory is the fact of giving flexibility in the model allowing us to develop a lot of algorithms close to the human thought [4].

An n-dimensional digital space Z^n is composed of a set of elements known as spels (Spatial Elements). In a three-dimensional space (n = 3) the elements are called voxels. Being the fuzzy relation ρ defined by $\rho = \{((x,y),\mu_\rho(x,y))|x,y \in Z^n\}$, where $\mu_\rho(x,y)$: $Z^n x Z^n \rightarrow [0,1]$ has a relation of relevance between each pair of elements belonging to the fuzzy object.

Fuzzy Connectivity involves two main concepts [9, 10]: adjacency and affinity. The relation of affinity $\mu_k(c,d)$ indicates the local similarity of intensity values of the spels and this consists of three properties: adjacency (μ_α), homogeneity (μ_ψ), and intensity (μ_ϕ) through the following identity: $\mu_k = \mu_\alpha(c,d).g(\mu_\psi(c,d),\mu_\phi(c,d))$. The relation of adjacency $\mu_\alpha(c,d)$, indicates the spatial proximity between the elements. We will consider c and d are neighbors, and then adjacency Fuzzy is unitary. Thus, the affinity equation is expressed as:

$$\mu_k = g(\mu_\psi(c,d),\mu_\phi(c,d)) \qquad (5)$$

Then, the calculation of affinity for each pair of spels c and d of a path $p_{c,d}$ is expressed by:

$$\mu_k(c,d) = w_1\mu_\phi(c,d) + w_2\mu_\psi(c,d) \qquad (6)$$

$$\mu_\psi(c,d) = \exp\left[-\frac{1}{2}\left(\frac{|f(c)-f(d)|-m_1}{s_1}\right)^2\right] \qquad (7)$$

$$\mu_\phi(c,d) = \exp\left[-\frac{1}{2}\left(\frac{\left(\frac{f(c)+f(d)}{2}\right)-m_2}{s_2}\right)^2\right] \qquad (8)$$

$$w_1 = \frac{\mu_\phi(c,d)}{\mu_\phi(c,d)+\mu_\psi(c,d)}, \quad w_2 = 1 - w_1 \qquad (9)$$

where m_1 and s_1 are the mean and standard deviation of the local homogeneity of the object. On the other hand, m_2 and s_2 are the mean and standard deviation of the intensities of the object, respectively. The weights w_1 and w_2 are adjusted for each pair of elements c and d belonging to the same path.

By combining the concepts of adjacency and affinity is possible to obtain the total connectivity for each pair of elements (c,d) consulted. If we take $p_{c,d} = \langle s_1, s_2, \ldots, s_N\rangle$ as a path between c and d, weaker affinity is the one that best represents this path and is given by [9, 10]:

$$\mu_K(p_{c,d}) = \min_{1<i<N}(\mu_k(s_{i-1}, s_i)) \qquad (10)$$

As there are finite paths between c and d, the best

representation of connectivity $\mu_K(c,d)$ selects the highest affinity between them as follows [9, 10]:

$$\mu_K(c,d) = max_{p \in P_{c,d}}(min_{1<i<N}(\mu_k(s_{i-1}, s_i))) \quad (11)$$

2.5. Process evaluation

Three parameters were used as evaluation metrics: True Positive (TP) rate and False Positive (FP) rate according to [12] and the Maximum Distance (Max_{dist}) [13] which gives an idea of the maximum shift or break off between the two images compared, $Max_{dist} = max|Cont_P - Cont_S|$.

3. Results

Table 2 presents consolidated evaluation results after the processing sequence for each of the simulated volumes and/or phantom of the left ventricle.

Table 2. Consolidation of the tests in the simulated left ventricular volumes and NCAT-4D phantom

Left Ventricle Simulated						
Volumes	Images with Poisson Noise			Images Filtered		
	TP (%)	FP (%)	Max_dist	TP (%)	FP (%)	Max_dist
Group I (Male)	91.40 ± 0.82	4.95 ± 0.40	5 pixels	98.40 ± 0.55	2.15 ± 0.18	2 pixels
Group I (Female)	92.41 ± 0.86	4.66 ± 0.54	4 pixels	98.43 ± 0.30	2.14 ± 0.21	2 pixels
Group I (Children)	92.44 ± 0.93	4.71 ± 0.70	4 pixels	98.49 ± 0.27	2.19 ± 0.19	2 pixels
Phantom NCAT-4D	91.51 ± 5.54	5.34 ± 1.23	5 pixels	94.05 ± 1.32	2.31 ± 0.93	2 pixels

4. Discussion and conclusion

It has been proven that the algorithm based on Fuzzy Connectedness theory is well suited for the segmentation of 3D images, and easily scalable to n-dimensions [9, 10].

Based on the results of the evaluation tests, performed on images without noise, it has been observed that the segmentation algorithm shows properly implemented functioning (approximately 100% for VP and 0% for FP).

The results using this methodology proved to be quite satisfactory. It has been obtained 2.19% of FP and 98.49% of TP at the end of the sequence of established processing.

It has been verified the importance of the filtering step as being an extremely prominent step for a more efficient phase of segmentation.

Under the idea of giving greater support to our processing framework, new input images will be used in future tests as more elaborate phantoms or real 3D PET images.

Acknowledgements

LEB-EPUSP (Biomedical Engineering Laboratory – Politecnical School of the University of São Paulo), **InCor** (Heart Institute of São Paulo - Brazil), **CNPq** (National Council of Scientific and Technological Development - Brazil), **MRE** (Ministério de Relações Exteriores Perú - Brasil).

References

[1] Adams E, Asua J, Conde OJ, Erlichman M, Flynn K, Hurtado-Saracho I. Positron Emission Tomography: Experience with PET and Synthesis of the Evidence. A Joint Project Produced on Behalf of: International Network of Agencies for Health Technology Assessment (INAHTA) 1999.

[2] Sabbatini R. The PET Scan: A New Window Into the Brain. Brain & Mind, Electronic Magazine on Neuroscience 1997.

[3] Sergars WP, Tsui BMW. MCAT TO XCAT: The Evolution of 4-D Computerized Phantoms for Imaging Research. IEEE 2009;97.

[4] Souza S, de Oliveira A. Alguns comentários sobre a Teoria Fuzzy. Matemática Aplicada IME – USP 1992;139- 147.

[5] Gonzales RC, Woods RE. Digital Image Processing. 3rd ed, New Jersey, Pearson Prentice Hall, 2008. Chap. 9 – Morphological Image Processing.

[6] Anscombe FJ. The transformation of Poisson, Binomial and Negative Binomial Dat. Biometrika 1948;15:246-254.

[7] Lee JS. Digital image enhancement and noise filtering by use of local statistics. IEEE Transactions on Pattern Analysis and Machine Intelligence 1980; PAMI-2:165-168.

[8] Inouye T. Square Root Transform for the Analysis of Quantum Fluctuationes in Spectrum Data. Nuclear Instruments and Methods 1970.

[9] Nyúl ALG, Falcão AX, Udupa JK. Fuzzy-connected 3D image segmentation at interactive speeds. Elsevier on Graphical Models 2002;64:259-281.

[10] Lage DM, Furuie SS. Visualização de artérias coronárias epicárdicas em imagens ecocardiográficas tridimensionais com contraste de microbolhas. Faculdade de Medicina da Universidade de São Paulo 2010.

[11] Computer Service of the Heart Institute of São Paulo (InCor – São Paulo).

[12] Udupa KJ, LaBlanc RV, Schmidt H. A Methodology for Evaluating Image Segmentation Algorithms 2002.

[13] Moraes MC, Furuie SS. Automatic coronary wall segmentation in intravascular ultrasound images using binary morphological reconstruction. Ultrasound in Medicine & Biology 2011;37:1486-1499.

Address for correspondence.
Name: Edward Flórez Pacheco
Postal address: Laboratório de Eng. Biomédica. Departamento de Telecomunicações e Controle. Escola Politécnica da Universidade de São Paulo. Av. Prof. Luciano Gualberto, Travessa 3, 158 – Sala D2-06. CEP 05508-970, SP – Brasil.
E-mail address: edward.florez@usp.br